

Specific Heat of Low Energy Spin Excitations at Elevated Temperatures Measured by Ferromagnetic Resonance

Benjamin W. Zingsem, Michael Winklhofer, Sabrina Masur, Paul Wendtland, Ruslan Salikhov, Florian M. Römer,

Ralf Meckenstock, Michael Farle

Faculty of Physics and Center for Nanointegration (CENIDE), University Duisburg-Essen, 47057 Duisburg, Germany

Abstract—We present ferromagnetic resonance (FMR) measurements on Fe thin films where the resonance condition is fulfilled in meta-stable magnetic states in saturation. By comparison to spin wave theory calculations, we show that a small deviation in the shape of the free energy surfaces between the point at which the metastable state is expected to disappear and the one at which it actually decays in the measurement is accounted for by the thermal energy of the magnonic and lattice system, namely the thermal fluctuation field. By comparison to the expected magnon heat capacity, we show that this finding offers the possibility to measure the magnonic contribution to the heat capacity by FMR independent of other contributions.

I. INTRODUCTION

Knowledge of the magnetic contribution to the thermal properties of physical systems is essential for the understanding of magnetocalorics and spintronics such as the spin Seebeck effect. Also for hyperthermia applications it is important to assess the coupling between the thermal properties of the magnetic contributions and the crystal system. Measuring the contribution of magnons to the heat capacity of magnetic materials at temperatures of technical interest however proves to be a difficult problem. It was shown in [1] that by using

fields of at least 30 T the magnon contribution in YIG can be suppressed in a temperature regime up to 20 K in order to separate it from other contributions. At higher temperatures the thermal properties are dominated by phonons. A suppressing field would need to be orders of magnitude higher than could be achieved technically, such that it becomes a challenging task to separate the magnon contribution. Here we propose a new method for determining the magnonic heat capacity using ferromagnetic resonance (FMR). The concept of our method is based on accurate angular dependent measurements around the magnetocrystalline hard axis of Fe films at a fixed microwave frequency. Using this unconventional FMR we have evaluated the Zeeman energy in critical configurations of metastable states. We show that in the temperature regime between 70 K and 280 K the temperature derivative of the critical Zeeman energy is proportional to the magnonic heat capacity.

II. EXPERIMENTAL PROCEDURE

In this study we perform ferromagnetic resonance measurements on an epitaxial 3 nmPt/2 nmAg/10 nmFe/10 nmAg/GaAs(001) thin film

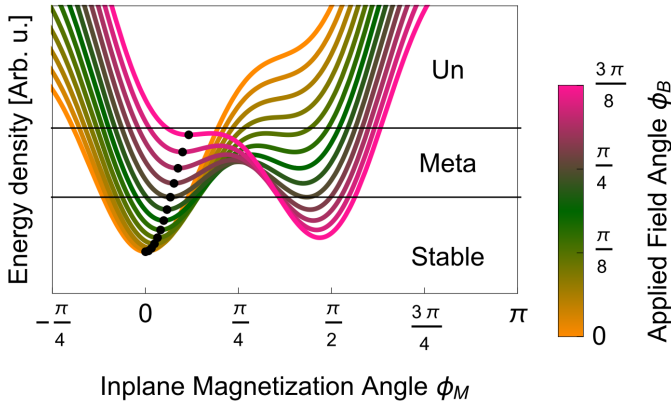


Figure 1. A plot of the energy landscape at different applied field angles for a fixed field strength. The black points illustrate the position of the minimum that determines the orientation of the magnetization. The unstable, metastable and stable regions for that state are separated by black lines. The unstable region can be regarded as non-existent in this example, as the formal minimum transitions into a saddle point rather than a maximum.

in which the (001)-direction of the Fe layer points out of the sample plane. For such systems the Helmholtz free energy density is known to have the form

$$F(\vec{B}, \vec{M}) = -\vec{M}(\theta, \phi) \cdot \vec{B}(\theta_B, \phi_B) + \frac{1}{2}\mu_0 M^2 \cos^2(\theta) + 2K_2^\perp \sin^2(\theta) + \frac{1}{4}K_4(\sin^2(2\theta) + \sin^4(\theta)\sin^2(2\phi)) \quad (1)$$

including the Zeeman contribution as discussed in [2]. The angles are given in spherical coordinates, where θ is the polar out-of-plane and ϕ the azimuthal in-plane angle.

In order for the magnetization to be resonantly excited it is necessary for $\vec{M}(\theta, \phi)$ to be a minimizer of this energy landscape. According to ref. this holds true, even if it is a local minimum. Thus the appearance of ferromagnetic resonant absorption is expected to occur in metastable states. In order to create such metastable states in the experiment, we sweep the angle of the applied field at fixed field strengths. The effect of such an angle sweep on the energy landscape at sufficiently low fields is shown in fig. 1. The metastable regime starts at an applied field angle of $\pi/4$ which corresponds to the hard direction of the energy landscape.

The experimental procedure for such an angle sweep is schematically shown in fig. 2. A sufficiently large field of 300 mT is applied along the magnetocrystalline easy axis of

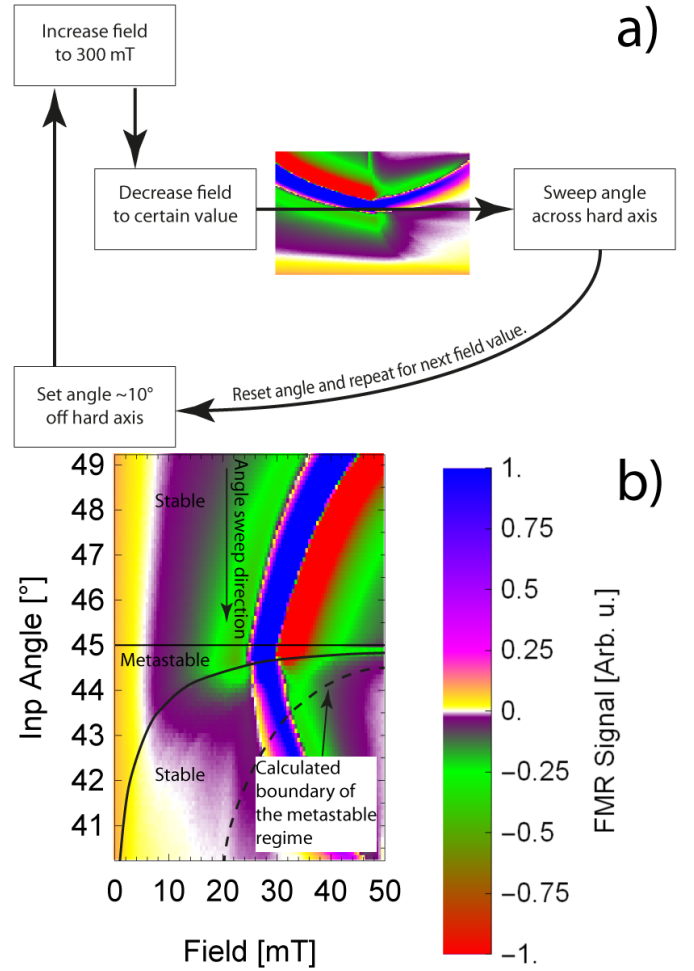


Figure 2. a) Schematic representation of the measurement procedure. b) Low field section of the measured FMR signal of a 10 nm Fe(100) film measured at 9.535 GHz at room temperature. The straight line at 45° indicates the magnetocrystalline hard direction, the curved line shows the critical angles at which the metastable regime ends and the dashed curved line indicates the boundary of the metastable regime as predicted using the theoretical model in ref. The difference between the black curve and the dashed curve along the horizontal axis corresponds to the thermal fluctuation field[3].

the sample to fully align the magnetization. Then the field is reduced to the desired field value for the angle sweep and the angle is swept from the easy axis across the hard axis in steps of 0.1° . One angle step takes about 0.3 s. During that sweep the FMR signal is recorded. The sharp discontinuity in the FMR signal that is indicated as a black line in fig. 2 pinpoints field-angle configurations at which the magnetization transitions from a metastable to a stable equilibrium. For the applied field magnitudes in this measurement we find, that this transition happens within a few degrees off the hard axis. These measurements were performed at various temperatures

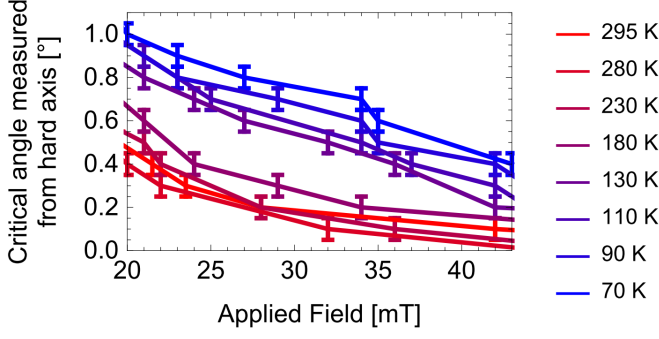


Figure 3. The boundary of the metastable regime for the sample measured in plane from the hard axis of the magnetocrystalline anisotropy. Points with error bars represent measured values, solid lines are linear interpolations used later to determine the temperature derivative at different fields.

and the curves that follow the measured of discontinuities at each temperature are depicted in fig. 3.

III. RESULTS AND DISCUSSION

We find, that as we decrease the temperature the critical angle offset from the hard axis at which the magnetization transitions from its metastable into a stable equilibrium increases and approaches the angle predicted for zero temperature as shown in fig. 3. The field regime from 20 mT to 43 mT was chosen because here the angles could be well distinguished and the sample is expected to be saturated.

For all temperatures the resonance field was extracted from the FMR spectra and fitted solving the commonly used eq. 2 [2], [4], [5], [6] to determine the anisotropy parameters.

$$\left(\frac{\omega}{\gamma}\right)^2 = \frac{1}{M^2 \sin^2(\theta)} \left(\frac{d^2}{d\theta^2} F \frac{d^2}{d\phi^2} F - \left(\frac{d^2}{d\theta d\phi} F \right)^2 \right) \quad (2)$$

For the fits, the experimental resonance field was used in the calculation to determine the orientation of the magnetization vector that minimizes the free energy density. This magnetization vector was then used in equation 2 to calculate the resonance field position for the respective frequency at a given set of anisotropy parameters. The so determined cubic anisotropy shown in fig. 4 is in agreement with literature data [2]. The out of plane uniaxial anisotropy K_2^\perp and the magnetization did not change significantly in the given tem-

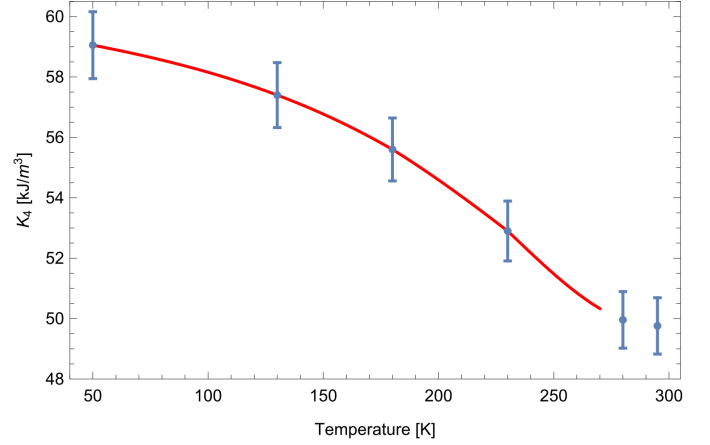


Figure 4. Cubic crystal anisotropy K_4 as a function of temperature. Blue points with error bars are the values obtained through fitting, the red curve is a third order polynomial interpolation to serve as a guide to the eye.

perature regime. We obtain $M = (1.71 \pm 0.01) \cdot 10^6$ A/m and $K_2^\perp = (16 \pm 0.6) \cdot 10^3$ J/m³, using a g factor of 2.09[7].

With these values we then evaluated the Zeeman contribution $F_{\text{Zeeman}} = -\vec{M} \cdot \vec{B}$ to the free energy density in eq. 1 for all temperatures using the critical angles ϕ_B from fig. 3 as the in plane applied field angle. In this calculation θ_B and θ are fixed to 90° due to the shape anisotropy of the sample. The magnetization angle ϕ is determined numerically by minimization eq. 1 within the metastable regime. This critical Zeeman energy density is the energy density that is provided to the system in order to perform the transition. Therefore we analyze its change as a function of temperature. Considering that the magnetization has some amount of heat available to it in the form of magnons we would expect, that as we decrease the temperature Zeeman energy is required to make the transition. Moreover since the Zeeman contribution is defined negative we expect that its change is proportional to the change of the magnon heat in the system. Therefore we calculated the change of the thermal energy of the magnons that is the heat capacity. To calculate the magnonic heat capacity we proceed as described in [8]. As of [9], [10] the magnon dispersion can be approximated as

$$\omega(k) = \gamma B + \omega_{ZB} \left(1 - \cos\left(\frac{\pi}{2} \frac{k}{k_m}\right) \right) \quad (3)$$

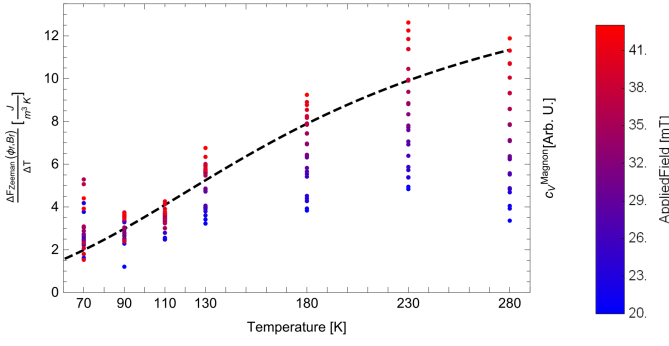


Figure 5. The red points show the central numerical derivative of the Zeeman contribution to the free energy including error bars. The black dashed curve is the result of numerically evaluating the magnon specific heat eq. 4. The parameters we used for Fe are $a = 286.65$ pm [12] $\omega_{ZB} = 18$ THz [8] $\gamma = 2.92 \cdot 10^{10}$ 1/T-s [7] and $\alpha_D = 0.87$ [11].

where γ is the magnetogyric ratio, B is the magnetic flux, $k_m = \alpha_D \frac{\sqrt[3]{6\pi^2}}{a}$ is the radius of the Debye-Sphere with the lattice constant a and the scaling factor α_D [11] that approximates the Brillouin zone and ω_{ZB} is the magnon frequency at the zone boundary. According to [8], the magnon specific heat can then be written as

$$c_V^{\text{magnon}} = \frac{1}{(2\pi)^3} \int_0^{k_m} d^3k \frac{(\hbar\omega(k))^2}{k_B T^2} \frac{\exp\left(\frac{\hbar\omega(k)}{k_B T}\right)}{\left(\exp\left(\frac{\hbar\omega(k)}{k_B T}\right) - 1\right)^2} \quad (4)$$

by calculating the temperature derivative of the inner energy of the magnons. A comparison between the temperature derivative of the Zeeman contribution and the numerically calculated magnon heat capacity of Fe is shown in fig. 5. We find, that for each applied field the curves are proportional which leads us to the conclusion, that this experiment offers a way to measure the heat capacity of magnons at elevated temperatures.

IV. SUMMARY

We have shown that non collinear FMR modes exist in metastable magnetic states as predicted in ref. . We also find that the magnonic heat capacity of iron is proportional to the temperature derivative of the Zeeman energy at the critical points in the unconventional FMR angular dependence by comparison to spin-wave theory calculations. We find a good agreement between the measured data and the calculation.

Further investigations will be conducted on different materials as well as microwave power dependent measurements.

REFERENCES

- [1] S. M. Rezende and J. C. López Ortiz, “Thermal properties of magnons in yttrium iron garnet at elevated magnetic fields,” *Phys. Rev. B*, vol. 91, p. 104416, Mar 2015. [Online]. Available: <http://link.aps.org/doi/10.1103/PhysRevB.91.104416>
- [2] M. Farle, “Ferromagnetic resonance of ultrathin metallic layers,” *Reports on Progress in Physics*, vol. 61, no. 7, p. 755, 1998. [Online]. Available: <http://stacks.iop.org/0034-4885/61/i=7/a=001>
- [3] S. Bance, H. Oezelt, T. Schrefl, M. Winklhofer, G. Hrkac, G. Zimanyi, O. Gutfleisch, R. F. L. Evans, R. W. Chantrell, T. Shoji, M. Yano, N. Sakuma, A. Kato, and A. Manabe, “High energy product in battenberg structured magnets,” *Applied Physics Letters*, vol. 105, no. 19, pp. –, 2014. [Online]. Available: <http://scitation.aip.org/content/aip/journal/apl/105/19/10.1063/1.4897645>
- [4] H. Suhl, “Ferromagnetic resonance in nickel ferrite between one and two kilomegacycles,” *Phys. Rev.*, vol. 97, pp. 555–557, Jan 1955. [Online]. Available: <http://link.aps.org/doi/10.1103/PhysRev.97.555.2>
- [5] J. Smit and H. G. Beljers, “Ferromagnetic resonance absorption in bafel2o19, a highly anisotropic crystal,” *Philips Research Reports*, vol. 10, pp. 113–130, 1955.
- [6] G. Giannopoulos, R. Salikhov, B. Zingsem, A. Markou, I. Panagiotopoulos, V. Psycharis, M. Farle, and D. Niarchos, “Large magnetic anisotropy in strained fe/co multilayers on aucu and the effect of carbon doping,” *APL Mater.*, vol. 3, no. 4, pp. –, 2015. [Online]. Available: <http://scitation.aip.org/content/aip/journal/aplmater/3/4/10.1063/1.4919058>
- [7] Z. Frait and R. Gemperle, “The g-factor and surface magnetization of pure iron along [100] and [111] directions,” *Le Journal de Physique Colloques*, vol. 32, no. C1, pp. C1–541, 1971.
- [8] C. Kittel, *Quantum theory of solids*. New York: Wiley, 1963.
- [9] R. Gross and A. Marx, *Festkörperphysik*. Oldenbourg Wissenschaftsverlag, 2012. [Online]. Available: <https://books.google.de/books?id=4BY31IukHI8C>
- [10] S. M. Rezende, R. L. Rodríguez-Suárez, R. O. Cunha, A. R. Rodrigues, F. L. A. Machado, G. A. Fonseca Guerra, J. C. Lopez Ortiz, and A. Azevedo, “Magnon spin-current theory for the longitudinal spin-seebeck effect,” *Phys. Rev. B*, vol. 89, p. 014416, Jan 2014. [Online]. Available: <http://link.aps.org/doi/10.1103/PhysRevB.89.014416>
- [11] S. M. Rezende, R. L. Rodríguez-Suárez, J. C. Lopez Ortiz, and A. Azevedo, “Thermal properties of magnons and the spin seebeck effect in yttrium iron garnet/normal metal hybrid structures,” *Phys. Rev. B*, vol. 89, p. 134406, Apr 2014. [Online]. Available: <http://link.aps.org/doi/10.1103/PhysRevB.89.134406>

- [12] P. Kohlhaas, R. Donner and N. Schmitz-Pranghe, “Über die temperaturabhängigkeit der gitterparameter von eisen, kobalt und nickel im bereich hoher temperaturen,” *Z. Angew. Phys.*, vol. 23, pp. 245–249, 1967.